Attitude Control for Fractionated Space Systems

Andrew J. Miller [*] **Frédéric Mazenc** [**] **Maruthi R. Akella** [***]

[*] *The University of Texas at Austin, Austin, TX 78705 USA (e-mail: andrew.miller@austin.utexas.edu)*
[**] *Laboratoire Des Signaux et Systèms, Gif-sur-Yvette, France (e-mail: frederic.mazenc@lss.supelec.fr)*
[***] *The University of Texas at Austin, Austin, TX 78705 USA (e-mail: makella@utexas.edu)*

Abstract: This paper addresses the attitude stabilization problem for fractionated space systems where the onboard computers cannot run continuously. An auxiliary filter is constructed to imitate the intermittent computer or state acquisition of a small size, power, and weight constrained spacecraft such a CubeSat. The proposed controller does not require angular rate or inertia knowledge and guarantees attitude stabilization and boundedness for all closed loop signals for persistently excited gains driving the auxiliary filter. A novel Lyapunov function is constructed to guarantee stability including auxiliary functions for strictification of the controller. Simulation of a 3U form factor CubeSat example is carried out to demonstrate the feasibility of the controller.

Keywords: Control under computation constraints, Lyapunov methods, Stability of nonlinear systems, Guidance, navigation and control of vehicles, Micro-nano-aerospace vehicles/satellites

1. INTRODUCTION

The cost of launching a satellite into space has decreased dramatically in the past decade. Despite the decreasing costs, satellite hardware is limited in the amount of computational resources, sensors, and actuators that are completely necessary for the mission. An extreme case of satellites with limited hardware is a fractionated space system where each subsystem is flown in physically disjoint/separate units that interact wirelessly, as in Brown and Eremenko (2008); Mathieu and Weigel (2006). A fractionated system can be expected to employ a separate (and offboard located) navigation subsystem that determines its state as well as the states of the other subsystems. State information from the navigation subsystem is sent to the communication subsystem and then distributed across the rest of the attitude determination and control subsystems. Communicating the states of all the subsystems cannot be done continuously due to power and computation constraints as well as the inability for the navigation subsystem to measure the state of the each subsystem simultaneously. Despite intermittent state information, there is still a need to control the attitude of each satellite in the fractionated system, even with limited computational resources.

A particular class of multi-spacecraft missions with limited computational resources arises within the context distributed satellite systems. These distributed satellite systems consist of several satellites (possibly heterogeneous) that communicate with each other, share goals in a cooperative way, and outperform capabilities of single satellite systems Poghosyana et al. (2016). Satellite systems consist of spacecraft with vastly different hardware, designed with each satellite performing its role for a specific part of the mission. It is advantageous to distribute the computational resources, communication bandwidth, and science equipment unevenly between the spacecraft, with the more capable spacecraft placed in a safer orbit while the more dispensable, less capable spacecraft collect data in a more dangerous environment. For example, Chen et al. (2022) has proposed a mothership-CubeSat radioscience mission of Phobos where the dispensable CubeSats are placed in an orbit close to Phobos while the mothership satellite carrying the majority of the computational resources remains in a high orbit. The mothership and CubeSats exchange two-way Doppler measurements to determine the exact orbits of the CubeSats as well as geodetic characteristics of Phobos. These smaller, less capable spacecraft often do not possess the sensors estimate their own state and rely on receiving state information from the mothership spacecraft. Receiving state information continuously is often not possible due to the power and computational limitations of the smaller spacecraft.

Computational limitations of small spacecraft pose a unique challenge when designing attitude controllers. The control law must maneuver a spacecraft in the presence of intermittent state information as well as intermittent periods to compute the control law. This work explores the problem of attitude stabilization for a spacecraft with an onboard computer that cannot be used all the time, but rather is available only intermittently, modulated by a persistently exciting (PE) signal. Srikant and Akella (2009) has addressed the problem of stabilizing a linear system with a persistently excited controller that is singular for finite periods of time. Sukumar and Akella (2012) has also addressed the problem of stabilizing a linear system where the observer gains are singular for finite periods of time. Another early paper Sukumar and Akella (2011) uses the notion of PE for intermittent actuation but assuming availability of both orientation and rate signals for feedback purposes. While these previous works handle a general linear dynamical system, this work presents results for a nonlinear system, the rigid body attitude stabilization problem. While there are some parallels between this formulation and that of anytime control, certain crucial differences exist between these approaches. In this work, we consider a continuous time problem where the control input is commanded through the control law, and does not involve calculating any open-loop optimal control input. Full state information is assumed to be available at all time rather than measuring the state at discrete times Zilberstein (1996). This paper proposes a control law that stabilizes a spacecraft with intermittent computational resources through the use of an auxiliary filter. The controller does not use angular rate measurements or require any knowledge of the spacecraft's inertia which is also a major distinction for this work compared to Srikant and Akella (2009); Sukumar and Akella (2011, 2012). Closed-loop stability is shown through Lyapunov analysis. Another major contribution is that strictification of the Lyapunov function is successfully accomplished which can provide the basis for further robustness analysis in face of sensing errors or the presence of unmodeled external disturbances.

2. PRELIMINARIES

For a positive definite matrix $P \in \mathbb{R}^{n\times n}$, let subscripts M and m denote the largest and smallest eigenvalues respectively, i.e., $P_M = |P|$ and $P_m = 1/|P^{-1}|$. Given a three dimensional vector $v = (v_1, v_2, v_3)^\top \in \mathbb{R}^3$, the cross product between v and another vector $w \in \mathbb{R}^3$ is equivalently expressed as $v \times w = v^* w$, where the skew-symmetric matrix $v^* \in \mathbb{R}^{3\times 3}$ is defined by

$$v^* = \begin{bmatrix} 0 & -v_3 & v_2 \\ v_3 & 0 & -v_1 \\ -v_2 & v_1 & 0 \end{bmatrix} . \tag{1}$$

Note that the equalities

$$\begin{aligned} v^{*\top} &= -v^* \ , \\ v^* w &= -w^* v \ , \\ w^* v^* &= v w^\top - w^\top v I_3 \ , \\ (w^* v)^* &= v w^\top - w v^\top \end{aligned}$$

and inequalities

$$\begin{aligned} |v^* Q v|^2 &\le (Q_M - Q_m)\,|v|^2 (v^\top Q v) \\ &\le Q_M (Q_M - Q_m) |v|^4 \end{aligned}$$

hold for all $v, w \in \mathbb{R}^3$ and positive semi-definite $Q \in \mathbb{R}^{3\times 3}$. The notation $|\cdot|$ is used to denote magnitude for scalar variables and the Euclidean norm for vectors and matrices.

3. PROBLEM STATEMENT

Consider the kinematics and rotational dynamics for a rigid-body expressed by

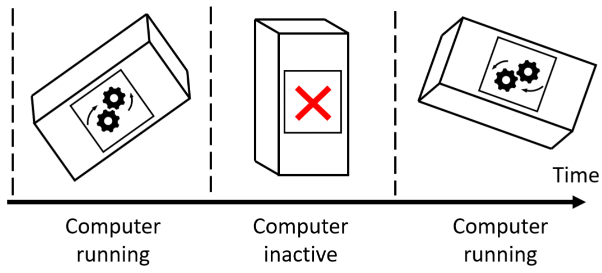

Fig. 1. Graphic of a CubeSat with a computer intermittently active.

$$\dot{s}(t) = \frac{1}{2} E(s(t))\omega(t) = \frac{1}{2} \begin{bmatrix} -q(t)^\top \\ q^*(t) + p(t) I_3 \end{bmatrix} \omega(t) \tag{2}$$

$$J\dot{\omega}(t) = -\omega^*(t) J \omega(t) + u(t) \tag{3}$$

where I_3 is the 3×3 identity matrix, $J > 0, J = J^\top \in \mathbb{R}^{3\times 3}$ is the inertia matrix, $s(t) = [p(t), q^\top(t)]^\top$ is the 4-dimensional quaternion parameterization for the rotational kinematics, $\omega(t) \in \mathbb{R}^3$ is the angular velocity vector expressed in a body-fixed frame of reference, and $u(t) \in \mathbb{R}^3$ is the external applied torque (the control signal). The unit-quaternion vector $s(t)$ satisfies the unit-norm constraint $|s(t)|^2 = p^2(t) + q^\top(t) q(t) = 1$ for all $t \ge 0$ with $p(t) \in \mathbb{R}$ and $q(t) \in \mathbb{R}^3$ respectively interpreted as the "scalar" and "vector" parts of the quaternion.

Let $\gamma(t)$ be the user-specified scalar signal. It is non-negative for all time $t \ge 0$, piecewise continuous, upper-bounded by a constant that we denote $\overline{\gamma}$, and is persistently exciting, i.e., there exist finite positive constants μ_1, μ_2, and T such that

$$\mu_2 \ge \int_t^{t+T} \gamma(\tau)\, d\tau \ge \mu_1 > 0$$

holds for all $t \ge 0$. The signal $\gamma(t)$ can be thought of as signaling when the onboard computer is active. Fig. 1 depicts the behavior of a CubeSat's computer that is not continuously operating.

Next, we construct a scalar dynamical system governed by

$$\dot{R}(t) = -\lambda R(t) + \gamma(t) \tag{4}$$

with $\lambda > 0$ and initial condition $R(0) > 0$. Recalling the result from Lemma 4 in Srikant and Akella (2009), it follows that there exists a strictly positive finite constant $\underline{R}$ such that $R(t) \ge \underline{R}$ for all $t \ge 0$. This ensures the auxiliary filter dynamics described by

$$\dot{\sigma}(t) = -\frac{\gamma(t)}{2R(t)} \left[\sigma(t) - s(t)\right] \tag{5}$$

is well-posed.

Note also that beyond boundedness and persistence of excitation, we place no further restrictions upon the signal $\gamma(t)$ such as analyticity or periodicity. When the onboard computer is unavailable, $\gamma = 0$ and (4) simply reduces to $R(t + \delta) = \exp(-\lambda t) R(\delta)$, for $t \ge \delta$ with δ representing the time-instant when the processor was last available before being turned off. Similarly, for $\gamma = 0$, (5) results in $\dot{\sigma}(t) = 0$ and thus, $\sigma(t)$ remains fixed at $\sigma(\delta)$ where again δ denotes the time-instant when the processor was last available.

The control objective is to design the input torque $u(t)$ using feedback of $[s(t), \sigma(t), R(t)]$ such that

$$\lim_{t\to\infty} |[(q(t), \omega(t), \sigma(t) - s(t))]| = 0 \quad (6)$$

while maintaining boundedness for all closed-loop signals. Toward achieving the stated control objective, we introduce the following non-negative function

$$V_0(t) = \mathsf{a}\left[(p(t)-1)^2 + |q(t)|^2\right] + \frac{1}{2}\omega^\top(t) J\omega(t) + R(t)\, |s(t) - \sigma(t)|^2 \quad (7)$$

where a is any user-specified positive constant. The time-derivative of $V_0(t)$ in (7) taken along (2), (3), (5), and (4) is given by

$$\dot{V}_0(t) = \omega(t)^\top \left[u(t) + \mathsf{a}q(t) + R(t)E^\top(s(t))(s(t) - \sigma(t))\right] - \lambda R(t)\, |s(t) - \sigma(t)|^2 \quad (8)$$

Thus, selecting

$$u(t) = -\mathsf{a}q(t) + R(t)E^\top(s(t))\sigma(t) \quad (9)$$

and using the fact that $E^\top(s(t))s(t) = 0$ holds for all $t \geq 0$, we have

$$\dot{V}_0(t) = -\lambda R(t)\, |s(t) - \sigma(t)|^2$$

It follows that

$$\dot{V}_0(t) \leq -\lambda \underline{R}\, |s(t) - \sigma(t)|^2 \quad (10)$$

Let us notice that the system (2)-(3) in closed-loop with the feedback (9) admits the representation:

$$\begin{aligned} \dot{s}(t) &= \frac{1}{2}E(s(t))\omega(t) \\ J\dot{\omega}(t) &= -\omega(t)^* J\omega(t) - \mathsf{a}q(t) + R(t)E(s(t))^\top \sigma(t) \end{aligned} \quad (11)$$

From (10) and the features of V_0, we deduce that $\omega(t)$ and $|s(t) - \sigma(t)|$ are bounded. Then from (5), we deduce that $\sigma(t)$ is bounded thereby ensuring boundedness for states of the resulting closed-loop system. Besides, (4) and the boundedness of $\gamma(t)$ ensures that R is bounded. Bearing in mind (11), we deduce that the time derivative of all the solutions of the closed-loop system are bounded. We deduce that all the solutions of the closed-loop system are uniformly continuous. Noticing that (10) implies that

$$V_0(0) \geq \lambda \underline{R} \int_0^t |s(m) - \sigma(m)|^2\, dm \quad (12)$$

for all $t \geq 0$, we deduce from Barbalat's lemma Khalil (2002) that $\lim_{t\to\infty} |s(t) - \sigma(t)| = 0$. Successive applications of Barbalat's lemma further result in achieving the convergence condition (6). The filter is required in the control law because the signal σ provides the necessary damping for the closed-loop system. Without implementing the signal σ and using only attitude feedback (i.e., $u(t) = -\mathsf{a}q(t)$), we cannot ensure that $\lim_{t\to\infty}[q(t), \omega(t)] = 0$.

4. STRICTIFICATION

The purpose of strictification is to turn the proposed non-strict Lyapunov function into a strict Lyapunov function Malisoff and Mazenc (2009). Strict and non-strict in this context means having a negative definite and semi-negative definite derivative, respectively, along system trajectories. The construction of the strict Lyapunov function can be used for robustness analysis as well as problems where only output measurement is available. In general, non-strict Lyapunov functions are not sufficient for robustness analysis due to their negative semi-definite derivatives becoming positive in the presence of small perturbations. The following procedure shows the construction of a strict Lyapunov function for the closed-loop system established in the previous section of the paper.

Let us introduce auxiliary functions:

$$\begin{aligned} N_1(t) &= q(t)^\top J\omega(t) \\ N_2(t) &= \frac{1}{2}\omega(t)^\top E(s(t))^\top [\sigma(t) - s(t)] \end{aligned} \quad (13)$$

Notice for later use that

$$N_2(t) = \dot{s}(t)^\top [\sigma(t) - s(t)] \quad (14)$$

Calculations give

$$\begin{aligned} \dot{N}_1(t) &= -\mathsf{a}|q(t)|^2 - q(t)^\top \omega(t)^* J\omega(t) \\ &\quad + R(t)q(t)^\top E(s(t))^\top \sigma(t) + \omega(t)^\top J\dot{q}(t) \\ &= -\mathsf{a}|q(t)|^2 - q(t)^\top \omega(t)^* J\omega(t) \\ &\quad + R(t)q(t)^\top E(s(t))^\top (\sigma(t) - s(t)) \\ &\quad + \frac{1}{2}\omega(t)^\top J[q^*(t) + p(t)I_3]\omega(t) \end{aligned} \quad (15)$$

Using $q(t)^\top \omega(t)^* = -(\omega(t)^* q(t))^\top = (q(t)^* \omega(t))^\top = -\omega(t)^\top q(t)^*$, we obtain

$$\begin{aligned} \dot{N}_1(t) &= -\mathsf{a}|q(t)|^2 + \omega(t)^\top q(t)^* J\omega(t) \\ &\quad + \frac{1}{2}\omega(t)^\top J[q^*(t) + p(t)I_3]\omega(t) \\ &\quad + R(t)q(t)^\top E(s(t))^\top (\sigma(t) - s(t)) \end{aligned} \quad (16)$$

Since $\omega(t)^\top q(t)^* J\omega(t) = -\omega(t)^\top Jq(t)^*\omega(t)$, we obtain

$$\begin{aligned} \dot{N}_1(t) &= -\mathsf{a}|q(t)|^2 + \frac{1}{2}\omega(t)^\top J[-q^*(t) + p(t)I_3]\omega(t) \\ &\quad + R(t)q(t)^\top E(s(t))^\top (\sigma(t) - s(t)) \\ &= -\mathsf{a}|q(t)|^2 + p(t)\omega(t)^\top J\omega(t) \\ &\quad - \frac{1}{2}\omega(t)^\top J[q^*(t) + p(t)I_3]\omega(t) \\ &\quad + R(t)q(t)^\top E(s(t))^\top (\sigma(t) - s(t)) \end{aligned} \quad (17)$$

Since $|q(t)^* + p(t)I_3| \leq 1$ and $|p(t)| \leq 1$ for all $t \geq 0$, the inequality

$$\begin{aligned} \dot{N}_1(t) \leq& -\mathsf{a}|q(t)|^2 + \frac{3|J|}{2}|\omega(t)|^2 \\ &+ R(t)q(t)^\top E(s(t))^\top (\sigma(t) - s(t)) \end{aligned} \quad (18)$$

holds. Let $\overline{R} > 0$ be a constant such that $R(t) \leq \overline{R}$ for all $t \geq 0$. Then

$$\dot{N}_1(t) \leq -\mathsf{a}|q(t)|^2 + \frac{3|J|}{2}|\omega(t)|^2 + \overline{R}|q(t)||\sigma(t) - s(t)| \quad (19)$$

because $|s(t)| = |E(s(t))| = 1$ for all $t \geq 0$.

The derivative of N_2 satisfies:

$$\begin{aligned} \dot{N}_2(t) &= \dot{s}(t)^\top [\dot{\sigma}(t) - \dot{s}(t)] + \ddot{s}(t)^\top [\sigma(t) - s(t)] \\ &= -|\dot{s}(t)|^2 - \dot{s}(t)^\top \frac{\gamma(t)}{2R(t)}[\sigma(t) - s(t)] \\ &\quad + \ddot{s}(t)^\top [\sigma(t) - s(t)] \end{aligned} \quad (20)$$

Since

$$\begin{aligned}\ddot{s}(t) &= \frac{1}{2}E(\dot{s}(t))\omega(t) + \frac{1}{2}E(s(t))\dot{\omega}(t) \\ &= \frac{1}{2}E\left(\frac{1}{2}E(s(t))\omega(t)\right)\omega(t) \\ &\quad + \frac{1}{2}E(s(t))J^{-1}[-\omega(t)^* J\omega(t) - \mathsf{a}q(t)] \\ &\quad + \frac{R(t)}{2}E(s(t))J^{-1}E(s(t))^\top \sigma(t) \\ &= -\frac{1}{4}|\omega(t)|^2 s(t) \\ &\quad + \frac{1}{2}E(s(t))J^{-1}[-\omega(t)^* J\omega(t) - \mathsf{a}q(t)] \\ &\quad + \frac{R(t)}{2}E(s(t))J^{-1}E(s(t))^\top \sigma(t)\end{aligned} \tag{21}$$

we obtain

$$\begin{aligned}\dot{N}_2(t) &= -|\dot{s}(t)|^2 - \dot{s}(t)^\top \frac{\gamma(t)}{2R(t)}[\sigma(t) - s(t)] \\ &\quad -\frac{1}{4}|\omega(t)|^2[\sigma(t)-s(t)]^\top s(t) \\ &\quad +\frac{1}{2}[\sigma(t)-s(t)]^\top E(s(t))J^{-1}[-\omega(t)^* J\omega(t)] \\ &\quad -\frac{1}{2}[\sigma(t)-s(t)]^\top E(s(t))J^{-1}\mathsf{a}q(t) \\ &\quad +\frac{R(t)}{2}[\sigma(t)-s(t)]^\top E(s(t))J^{-1}E(s(t))^\top \sigma(t) \\ &\quad -\frac{R(t)}{2}[\sigma(t)-s(t)]^\top E(s(t))J^{-1}E(s(t))^\top s(t)\end{aligned} \tag{22}$$

Let $\overline{\aleph} = \frac{\overline{\gamma}}{2\underline{R}}$. Then $\frac{\gamma(t)}{2R(t)} \leq \overline{\aleph}$ for all $t \geq 0$. Now, observe that $|\dot{s}(t)|^2 = \frac{1}{4}|\omega(t)|^2$ and $|s(t)| = |E(s(t))| = 1$ for all $t \geq 0$. We deduce that

$$\begin{aligned}\dot{N}_2(t) &\leq -\frac{1}{4}|\omega(t)|^2 - \frac{\gamma(t)}{2R(t)}\dot{s}(t)^\top[\sigma(t)-s(t)] \\ &\quad +\frac{1}{4}|\omega(t)|^2|\sigma(t)-s(t)| \\ &\quad +\frac{J^\sharp}{2}|\sigma(t)-s(t)||\omega(t)^* J\omega(t) + \mathsf{a}q(t)| \\ &\quad +\frac{\overline{R}J^\sharp}{2}|\sigma(t)-s(t)|^2 \\ &\leq -\frac{1}{4}|\omega(t)|^2 + \frac{\overline{\aleph}}{2}|\omega(t)||\sigma(t)-s(t)| \\ &\quad +\frac{1}{4}|\omega(t)|^2|\sigma(t)-s(t)| \\ &\quad +\frac{J^\sharp}{2}|\sigma(t)-s(t)||\omega(t)^* J\omega(t) \\ &\quad +\mathsf{a}q(t)| + \frac{\overline{R}J^\sharp}{2}|\sigma(t)-s(t)|^2\end{aligned} \tag{23}$$

with $J^\sharp = |J^{-1}|$. Thus

$$\begin{aligned}\dot{N}_2(t) &\leq -\frac{1}{4}|\omega(t)|^2 + \frac{\overline{\aleph}}{2}|\omega(t)||\sigma(t)-s(t)| \\ &\quad +\left(\frac{1}{4} + \frac{J^\sharp|J|}{2}\right)|\omega(t)|^2|\sigma(t)-s(t)| \\ &\quad +\frac{J^\sharp\mathsf{a}}{2}|q(t)||\sigma(t)-s(t)| \\ &\quad +\frac{\overline{R}J^\sharp}{2}|\sigma(t)-s(t)|^2\end{aligned} \tag{24}$$

Let us introduce the auxiliary function:

$$S(t) = N_1(t) + 2(3|J|+1)N_2(t) \tag{25}$$

Then from the inequalities (18) and (24), we deduce that

$$\begin{aligned}\dot{S}(t) &\leq -\mathsf{a}|q(t)|^2 - \frac{1}{2}|\omega(t)|^2 + \mathfrak{b}_1|q(t)||\sigma(t)-s(t)| \\ &\quad +\mathfrak{b}_2|\omega(t)||\sigma(t)-s(t)| \\ &\quad +\mathfrak{b}_3|\omega(t)|^2|\sigma(t)-s(t)| + \mathfrak{b}_4|\sigma(t)-s(t)|^2\end{aligned} \tag{26}$$

with $\mathfrak{b}_1 = \overline{R} + (3|J|+1)J^\sharp\mathfrak{a}$, $\mathfrak{b}_2 = (3|J|+1)\overline{\aleph}$, $\mathfrak{b}_3 = (3|J|+1)\left(\frac{1}{2} + J^\sharp|J|\right)$ and $\mathfrak{b}_4 = (3|J|+1)\overline{R}J^\sharp$. As an immediate consequence,

$$\begin{aligned}\dot{S}(t) &\leq -\frac{\mathsf{a}}{2}|q(t)|^2 - \frac{1}{4}|\omega(t)|^2 \\ &\quad + \left(\mathfrak{b}_5 + 2\mathfrak{b}_3^2|\omega(t)|^2\right)|\sigma(t)-s(t)|^2\end{aligned} \tag{27}$$

with $\mathfrak{b}_5 = \frac{\mathfrak{b}_1^2}{2} + 2\mathfrak{b}_2^2 + \mathfrak{b}_4$.

Now, let us consider the function:

$$U(t) = S(t) + \mathfrak{b}_6\left(\frac{1}{2}V_0(t)^2 + V_0(t)\right) \tag{28}$$

where $\mathfrak{b}_6 > 0$ is a parameter to be chosen later. Then (10) and (27) give

$$\begin{aligned}\dot{U}(t) &\leq -\frac{\mathsf{a}}{2}|q(t)|^2 - \frac{1}{4}|\omega(t)|^2 \\ &\quad + \left(\mathfrak{b}_5 + 2\mathfrak{b}_3^2|\omega(t)|^2\right)|\sigma(t)-s(t)|^2 \\ &\quad -\mathfrak{b}_6\left(V_0(t)+1\right)\lambda R(t)|s(t)-\sigma(t)|^2 \\ &\leq -\frac{\mathsf{a}}{2}|q(t)|^2 - \frac{1}{4}|\omega(t)|^2 \\ &\quad + \left(\mathfrak{b}_5 + 2\mathfrak{b}_3^2|\omega(t)|^2\right)|\sigma(t)-s(t)|^2 \\ &\quad -\mathfrak{b}_6\lambda\underline{R}\left[\frac{1}{2}\omega^\top(t)J\omega(t)\right]|s(t)-\sigma(t)|^2 \\ &\quad -\mathfrak{b}_6\lambda\underline{R}\left[\underline{R}\,|s(t)-\sigma(t)|^2 + 1\right]|s(t)-\sigma(t)|^2 \\ &\leq -\frac{\mathsf{a}}{2}|q(t)|^2 - \frac{1}{4}|\omega(t)|^2 \\ &\quad + [\mathfrak{b}_5 + 2\mathfrak{b}_3^2|\omega(t)|^2 \\ &\quad -\mathfrak{b}_6\lambda\underline{R}\left(\frac{J_m}{2}|\omega(t)|^2 + 1\right)|\sigma(t)-s(t)|^2\end{aligned} \tag{29}$$

where $J_m > 0$ is the smallest eigenvalue of J.

Choosing

$$\mathfrak{b}_6 \geq \max\left\{\frac{\mathfrak{b}_5+1}{\lambda\underline{R}}, \frac{4\mathfrak{b}_3^2+2}{\lambda\underline{R}J_m}\right\} \tag{30}$$

the inequality

$$\begin{aligned}\dot{U}(t) &\leq -\frac{\mathsf{a}}{2}|q(t)|^2 - \frac{1}{4}|\omega(t)|^2 \\ &\quad -\frac{\mathfrak{b}_6\lambda\underline{R}}{2}\left(|\omega(t)|^2+1\right)|s(t)-\sigma(t)|^2\end{aligned} \tag{31}$$

is satisfied. Now, let us observe that

$$V_0(t) \geq \mathsf{a}\,|q(t)|^2 + \frac{J_m}{2}|\omega(t)|^2 + \underline{R}\,|s(t)-\sigma(t)|^2 \tag{32}$$

and

$$\begin{aligned}|S(t)| &\leq |J||q(t)||\omega(t)| \\ &\quad +2(3|J|+1)\left|\frac{1}{2}E(s(t))\omega(t)\right||\sigma(t)-s(t)| \\ &\leq |J||q(t)||\omega(t)| \\ &\quad +(3|J|+1)|\omega(t)||\sigma(t)-s(t)| \\ &\leq \frac{1}{2}|J||q(t)|^2 + \frac{4|J|+1}{2}|\omega(t)|^2 \\ &\quad +\frac{3|J|+1}{2}|\sigma(t)-s(t)|^2\end{aligned} \tag{33}$$

We deduce from

$$|S(t)| \leq \mathfrak{c}\left[\mathsf{a}\,|q(t)|^2 + \frac{J_m}{2}|\omega(t)|^2 + \underline{R}\,|s(t)-\sigma(t)|^2\right] \tag{34}$$

with

$$\mathfrak{c} = \max\left\{\frac{|J|}{2\mathsf{a}}, \frac{4|J|+1}{J_m}, \frac{3|J|+1}{2\underline{R}}\right\} \tag{35}$$

From (34) and (32), we deduce that

$$|S(t)| \leq \mathfrak{c}V_0(t) \tag{36}$$

Thus, choosing

$$\mathfrak{b}_6 \geq 2\mathfrak{c} \tag{37}$$

the inequality

$$U(t) \geq \frac{\mathfrak{b}_6}{2}\left(\frac{1}{2}V_0(t)^2 + V_0(t)\right) \tag{38}$$

is satisfied.

The conditions (37) and (30) give the following condition:

$$\mathfrak{b}_6 \geq \max\left\{\frac{\mathfrak{b}_5+1}{\lambda\underline{R}}, \frac{4\mathfrak{b}_3^2+2}{\lambda\underline{R}J_m}, \frac{|J|}{\mathsf{a}}, 2\frac{4|J|+1}{J_m}, \frac{3|J|+1}{\underline{R}}\right\} \tag{39}$$

The strictification of the Lyapunov function aids in the analysis of several other considerations such as uncertainty in system parameters, input perturbations as well as control degradation.

5. SIMULATION RESULTS

A simulation of a 3U CubeSat is carried out with the proposed controller. The goal is to stabilize the CubeSat by bringing it to rest $\omega = [0,0,0]^\top$(rad/s) and to the desired final orientation $s = [1,0,0,0]^\top$. The initial angular velocity of the CubeSat is $\omega(0) = [0.1, 0.1, -0.1]^\top$(rad/s) and the quaternion describing the initial orientation is $s(t) = [\sqrt{2}/2, -0.5, 0, 0.5]^\top$. The moment of inertia for the 4kg CubeSat is $J = \text{diag}[0.0416, 0.0083, 0.0416](\text{kgm}^2)$. The constant in the scalar dynamical system is $\lambda = 0.1$. The proportional gain parameter is $a = 2$, and the user defined signal is

$$\gamma(t) = \begin{cases} 1, & 0 \leq t < \alpha T \\ 0, & \alpha T \leq t < T \end{cases} \tag{40}$$

and periodic continuation. The parameter $T = 20(s)$ is the period of the user defined signal and $\alpha = 0.5$ is the fraction of the period when the signal is unity. The signal is meant to imitate the onboard computer limiting its use due to power constraints. Fig 2 and Fig 3 show the 2-norm of the CubeSat's attitude and angular velocity respectively, over time.

Fig 4 shows the 2-norm of the difference between the auxiliary filter $\sigma(t)$ and the quaternion $s(t)$ over time. The auxiliary filter $\sigma(t)$ tracks and converges to the true value of the quaternion exponentially fast, as expected. Simulations with different values of the control gain a were carried out. Choosing the proportional gain greater or less than 10 times $a = 2$ increased and decreased the maximum commanded torque respectively, but offered no increase in rate of convergence of the state variables. Instead, choosing the proportional gain greater or less than 10 times $a = 2$ decreased the rate of convergence. Unlike with a proportional derivative controller, the proportional gain a does not explicitly appear in the decay rate of the Lyapunov function in (10). Therefore, it is not explicit in the derivation that increasing the proportional gain will increase rate of convergence. Simulations were also carried out for different values of α. Fig 5 shows the 2-norm of the difference between the auxiliary filter $\sigma(t)$ and the quaternion $s(t)$ over time for the case of $\alpha = 0.1$, the on-board computer active for two seconds every $T = 20(s)$. As expected, the filter takes longer to converge to the true value of the quaternion when the user defined signal is

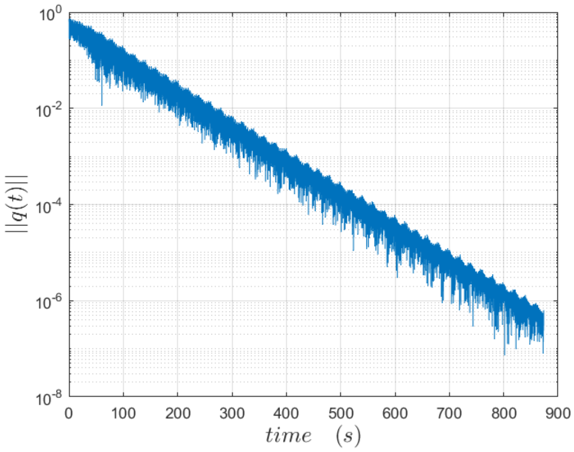

Fig. 2. Plot of the 2-norm of the vector quaternion over time.

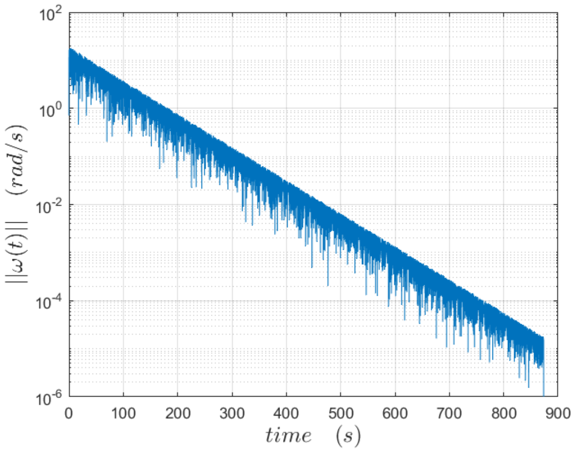

Fig. 3. Plot of the 2-norm of the angular velocity over time.

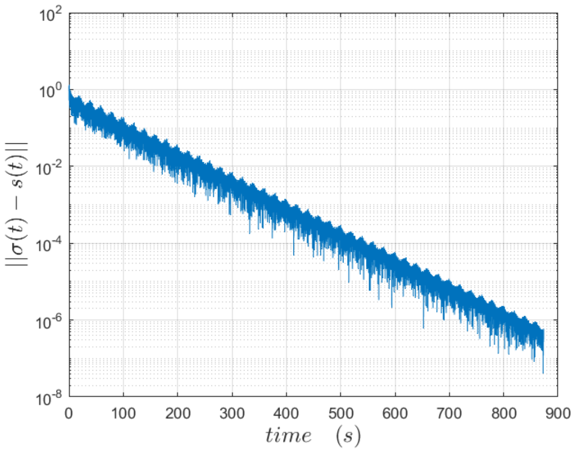

Fig. 4. Plot of the 2-norm of the difference of the auxiliary filter and quaternion.

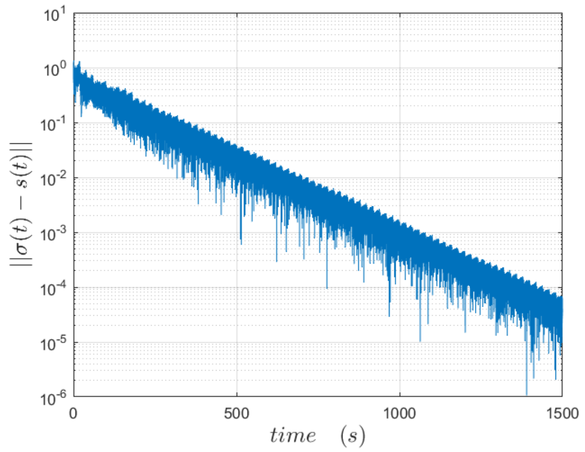

Fig. 5. Plot of the 2-norm of the difference of the auxiliary filter and quaternion.

unity for a smaller amount of time. Fig 6 shows the 2-norm of the CubeSat's attitude over time for the case of $\alpha = 0.1$. The rate of convergence of the quaternion is smaller for the

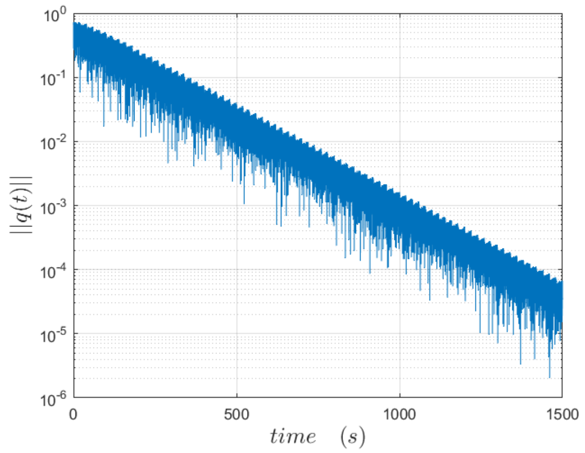

Fig. 6. Plot of the 2-norm of the vector quaternion over time.

smaller value of α. Regardless of the values of a and α, the proposed controller is able to stabilize the CubeSat with a PE auxiliary filter.

6. CONCLUSION

This paper addresses the attitude stabilization problem for spacecraft with on-board computers that are not constantly running, but rather persistently excited. Scenarios for attitude stabilization with persistently excited computers include fractionated space systems and distributed satellite systems with low capability satellites in dangerous environments. An auxiliary filter is created where the filter dynamics are inactive for periods of time, to mirror the persistently excited computer. The auxiliary state is used in the control law, which is shown to stabilize the spacecraft even when there are periods of time when the auxiliary dynamics are inactive. Simulation results show the proposed controller stabilizes the spacecraft while the auxiliary filter is active only a faction of the time. The proposed control law is not entirely governed by the user defined signal that imitates the on-board computer because the quaternion is directly used in the control law. However, this work is a starting point for developing a full persistently excited attitude controller. Future work includes extending the persistently excited component of the controller to the entire attitude control law, as well as using higher fidelity models of the on-board computer.

REFERENCES

Brown, O. and Eremenko, P. (2008). Application of value-centric design to space architectures: the case of fractionated spacecraft. In *AIAA SPACE 2008 conference & exposition*, 7869.

Chen, H., Rambaux, N., Lainey, V., and Hestroffer, D. (2022). Mothership-cubesat radioscience for phobos geodesy and autonomous navigation. *Remote Sensing*, 14.

Khalil, H.K. (2002). Nonlinear systems third edition. *Prentice Hall*, 115.

Malisoff, M. and Mazenc, F. (2009). *Constructions of strict Lyapunov functions*. Springer Science & Business Media.

Mathieu, C. and Weigel, A. (2006). Assessing the fractionated spacecraft concept.

Poghosyana, A., Llucha, I., Matevosyana, H., Lamba, A., Morenoa, C., Taylora, C., Golkara, A., Coteb, J., Mathieub, S., Pierottib, S., et al. (2016). Unified classification for distributed satellite systems. In *4th International Federated and Fractionated Satellite Systems Workshop, Rome, Italy*.

Srikant, S. and Akella, M. (2009). Persistence filter-based control for systems with time-varying control gains. *Systems Control Letters*, 58(6), 413–420.

Sukumar, S. and Akella, M.R. (2011). Precision attitude stabilization: Incorporating rise and fall times in gas-based thrusters. *journal of Guidance, Control, and Dynamics*, 34(1), 317–323.

Sukumar, S. and Akella, M.R. (2012). Persistence filters for estimation: Applications to control in shared-sensing reversible transducer systems. *Journal of Dynamic Systems, Measurement, and Control*, 134(4).

Zilberstein, S. (1996). Using anytime algorithms in intelligent systems. *AI magazine*, 17(3), 73–73.